Free vibration analysis of composite plates based on a variable separation method

Philippe Vidal, Laurent Gallimard, Olivier Polit

Free vibration analysis of composite plates based on a variable separation method

P. Vidal[*], L. Gallimard, O. Polit

LEME, UPL, Univ Paris Nanterre, F92410 Ville d'Avray, France

A R T I C L E   I N F O

A B S T R A C T

This work deals with the free vibration analysis of laminated composite plates through a variable separation approach. The displacement field is approximated as a sum of separated functions of the in-plane coordinates x, y and the transverse coordinate z. This choice yields to a non-linear problem that can be solved by an iterative process. That consists of solving a 2D and 1D eigenvalue problem successively. In the thickness direction, a fourth-order expansion in each layer is considered. For the in-plane description, classical Finite Element method is used.

A wide range of numerical tests involving several representative laminated and sandwich plates is addressed to show the accuracy of the present LayerWise (LW) method. Different slenderness ratios and boundary conditions are also considered. By comparing with exact or 3D FEM solutions, it is shown that it can provide accurate results less costly than classical LW computations.

1. Introduction

Nowadays, the composite and sandwich materials are no more confined to secondary structures, but they are also used for the primary ones. Thus, it calls for efficient and accurate numerical tools to design and ensure the suitable reliability. To achieve this purpose, this topics has been the focus of attention of many researchers during the past few years, in particular for the free vibration analysis. Various theories in mechanics for composite or sandwich structures have been developed and can be classified as:

- The Equivalent Single Layer (ESL) model: the different layers are homogeneized into only one equivalent layer. Thus, the number of unknowns is independent of the number of layers. It includes the classical plate theories, such as the Kirchhoff plate theory (CPT), Reissner-Mindlin [1,2] (first-order shear deformation theory, FSDT). Higher order shear deformation theories (HSDT) are also introduced to improve the description of the transverse shear stress through the thickness [3]. A particular warping function is included in some of them allowing to fulfill the free boundary conditions on the top and bottom surface of the laminates [4–9]. This type of model can be easily enhanced by using the so-called Murakami's zig-zag function as in [10]. To extend the capability of the HSDT models, the transverse normal stress can also be included in the formulation such as in [11–13].
- The LayerWise model (LW): it aims at overcoming the restriction of the ESL concerning the discontinuity of out-of-plane stresses on the interface layers and taking into account the specificity of layered structure. But, the number of degrees of freedom (dofs) depends on the number of layers. It was widely developed by Reddy [8,14,15] and also in [16,17]. Note the mixed approach addressed in [18].

These two families of models have been gathered into the so-called Carrera's Unified Formulation (CUF) [19] with a displacement-based or Reissner's Mixed Variational Theorem (RMVT) formulation. Then, CUF was extended to deduce the Generalized Unified Formulation (GUF) [20,21] and the Sublaminate Generalized Unified Formulation (SGUF) [22] in which the order of expansion for each displacement/transverse stress component can be chosen independently.

As an alternative, refined models have been developed in order to improve the accuracy of ESL models avoiding the additional computational cost of LW approach. The consideration of the continuity of the transverse shear stresses at the interfaces between the layers allows to derive the so-called zig-zag models. The interested readers can refer to [23,9,24–27].

A partial aspect of the broad research activity about models for layered structures is given herein. More complete reviews on the models, in particular in the vibration analysis framework, can be found

---

[*] Corresponding author.
E-mail address: philippe.vidal@parisnanterre.fr (P. Vidal).

in [28–32].

Over the past years, some methods based on the separation of variables have shown interesting features to model such types of structures. On the one hand, Kerr has extended the Kantorovich method (EKM) by considering it as only a first step of an iterative procedure [33,34]. A semi-analytic approach is deduced by considering the separation of the two in-plane spatial variables of the plate. The free vibration analysis is carried out in [35] for composite plates including only one term for the solution, while several couples are considered in [36] for isotropic plates. In these studies, a iterative process in which two successive eigenvalue problems are solved, is performed. Note that the composite plate models involving in the latter are based on a FSDT and HSDT (Reddy's model) theory. A more complete review of the applications of the EKM approach can be found in [37]. On the other hand, the Proper Generalized Decomposition (PGD) has been widely developed since the works of Ladevèze in the Latin framework [38] and Chinesta [39–41] for the model reduction. It has been successfully used in the context of the separation of in-plane/ out-of-plane coordinate variables for the static analysis of composite structures in [42–46]. The present work belongs to this latter family and is an extension towards the free vibration analysis. In this way, the displacements are written under the form of a sum of products of bidimensional polynomials of (x,y) and unidimensional polynomials of z. A piecewise fourth-order Lagrange polynomial of z is chosen and a 2D eight-node quadrilateral FE is employed for the in-plane coordinates. Each unknown function of (x,y) is classically approximated using one degree of freedom (dof) per node of the mesh and the LW unknown functions of z are global for the whole plate. Finally, the deduced non-linear problem implies the resolution of two eigenvalue problems alternatively. This process yields to a sequence of low-dimensional problems (2D and 1D) in which the number of unknowns is smaller than a classical Layerwise approach. For the present scope, only one or two couples will be considered. The later will be built simultaneously, without the use of a greedy algorithm as it is carried out in [47,48]. In these two works, only the lowest eigenvalue of the involved problem is determined. It should be noted that the interesting feature of the present approach lies on the possibility to have a higher-order z-expansion and to refine the description of the mechanical quantities through the thickness without increasing the computational cost. This is particularly suitable for the modeling of composite structures.

We now outline the remainder of this article. First, the classical mechanical formulation for the free vibration analysis is recalled. Then, it is applied in the particular framework of the PGD dedicated to the composite plate. The particular assumption on the displacements yields a non-linear problem. An iterative process is chosen to solve this one. The FE discretization is also described. Then, numerical tests are performed to show the performance and the limitations of the method. A convergence study is first proposed to illustrate the behavior of the approach to capture different modes and the associated natural frequencies. Then, the modeling of various representative laminated and sandwich plates is addressed. The influence of the slenderness ratio, the degree of anisotropy and boundary conditions is studied. Finally, an illustration of the computational cost is proposed to show the efficiency of the method when compared to the classical Layerwise approach. The assessment of the results is made by comparing with exact solutions, 3D FEM, quasi-3D results (displacement-based approach with a fourth-order Layerwise expansion LD4) and results available in open literature.

2. Reference problem description: the governing equations

Let us consider a composite plate structure occupying the domain $\mathscr{V} = \Omega \times \Omega_z$ where $\Omega = [0, a] \times [0, b]$ (a, b being the dimensions of the plate) and $\Omega_z = \left[-\frac{h}{2}, \frac{h}{2} \right]$ in a Cartesian coordinate (x, y, z). h is the thickness of the plate, see Fig. 1.
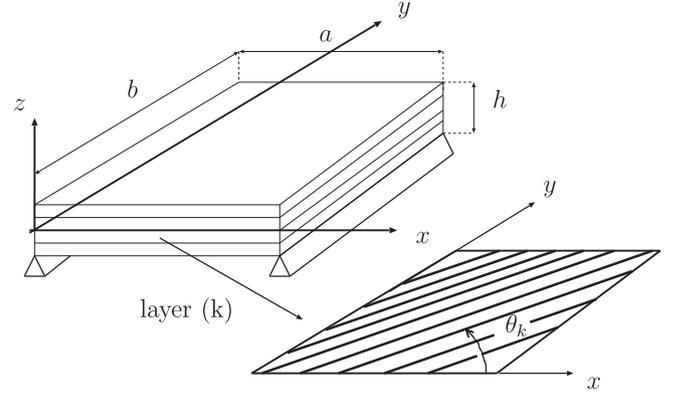

Fig. 1. Geometry of the plate and orientation of the fibers of the laminated plate.

2.1. Constitutive relation

The plate can be made of NC perfectly bonded orthotropic layers. The constitutive equations for a layer k can be written as

$$\sigma^{(k)} = \mathbf{C}^{(k)} \varepsilon \tag{1}$$

where we denote the stress vector by σ, the strain vector via ε.

We have

$$\mathbf{C}^{(k)} = \begin{bmatrix} C_{11}^{(k)} & C_{12}^{(k)} & C_{13}^{(k)} & 0 & 0 & C_{16}^{(k)} \\ & C_{22}^{(k)} & C_{23}^{(k)} & 0 & 0 & C_{26}^{(k)} \\ & & C_{33}^{(k)} & 0 & 0 & C_{36}^{(k)} \\ & & & C_{44}^{(k)} & C_{45}^{(k)} & 0 \\ & sym & & & C_{55}^{(k)} & 0 \\ & & & & & C_{66}^{(k)} \end{bmatrix} \tag{2}$$

where $C_{ij}^{(k)}$ are the three-dimensional stiffness coefficients of the layer (k).

Note that this 3D constitutive law is used in the present formulation.

2.2. The weak form of the boundary value problem

In the present study, the surface force density and the body force density are not considered. Considering the vibration problem, the displacement $\mathbf{d}(x, y, z, t)$ is assumed to be written as $\mathbf{d}(x, y, z, t) = \exp(\omega t)\mathbf{u}(x, y, z)$. We assume that a prescribed displacement $\mathbf{u} = 0$ is imposed on Γ_D.

Using the above matrix notations and for admissible displacement $\delta \mathbf{u} \in \delta U$, the variational principle is given by: find $\mathbf{u} \in U$ such that:

$$\int_{\mathscr{V}} \varepsilon(\delta \mathbf{u})^T \sigma \, d\mathscr{V} = \omega^2 \int_{\mathscr{V}} \rho \, \delta \mathbf{u}^T \mathbf{u} \, d\mathscr{V}, \quad \forall \, \delta \mathbf{u} \in \delta U \tag{3}$$

where U is the space of admissible displacements, i.e. $U = \{\mathbf{u} \in (H^1(\mathscr{V}))^3 / \mathbf{u} = \mathbf{0} \text{ on } \Gamma_D\}$. We have also $\delta U = \{\mathbf{u} \in (H^1(\mathscr{V}))^3 / \mathbf{u} = 0 \text{ on } \Gamma_D\}$. ρ is the mass density.

This problem can be expressed as

$$a(\mathbf{u}, \delta \mathbf{u}) = 0 \quad \forall \, \delta \mathbf{u} \in \delta \mathscr{W} \tag{4}$$

with

$$a(\mathbf{u}, \delta \mathbf{u}) = \int_{\Omega \times \Omega_z} \varepsilon(\delta \mathbf{u})^T \mathbf{C} \varepsilon(\mathbf{u}) \, d\Omega \, d\Omega_z - \omega^2 \int_{\Omega \times \Omega_z} \rho \, \delta \mathbf{u}^T \mathbf{u} \, d\Omega \, d\Omega_z \tag{5}$$

3. Application of the separated representation to the plate

In this section, we introduce the application of the variables separation for composite and sandwich plate for the vibration analysis. This specific separation has shown interesting features in the framework of static analysis [43,45]. The separated formulation is briefly

introduced in the subsequent sections.

3.1. The displacement and the strain field

The displacement solution $\mathbf{u}$ is constructed as the sum of N products of separated functions ($N \in \mathbb{N}^+$ is the order of the representation)

$$\mathbf{u}(x, y, z) = \sum_{i=1}^{N} \mathbf{f^i}(z) \circ \mathbf{v}^i(x, y) \tag{6}$$

where $\mathbf{f^i}(z)$ and $\mathbf{v}^i(x, y)$ are unknown functions which must be computed during the resolution process. $\mathbf{f^i}(z)$ and $\mathbf{v}^i(x, y)$ are defined on Ω_z and Ω respectively. The "$\circ$" operator in Eq. (6) is Hadamard's element-wise product. We have:

$$\mathbf{f^i} \circ \mathbf{v}^i = \mathbf{v}^i \circ \mathbf{f^i} = \begin{bmatrix} f_1^i(z) v_1^i(x, y) \\ f_2^i(z) v_2^i(x, y) \\ f_3^i(z) v_3^i(x, y) \end{bmatrix} \quad \text{with} \quad \mathbf{v}^i = \begin{bmatrix} v_1^i(x, y) \\ v_2^i(x, y) \\ v_3^i(x, y) \end{bmatrix} \quad \mathbf{f^i} = \begin{bmatrix} f_1^i(z) \\ f_2^i(z) \\ f_3^i(z) \end{bmatrix} \tag{7}$$

The strain can be expressed with respect to the reference frame in which the dependance with respect to the space coordinates is omitted as follows:

$$\varepsilon(u) = \sum_{i=1}^{N} \begin{bmatrix} f_1^i v_{1,1}^i \\ f_2^i v_{2,2}^i \\ (f_3^i)' v_3^i \\ (f_2^i)' v_2^i + f_3^i v_{3,2}^i \\ (f_1^i)' v_1^i + f_3^i v_{3,1}^i \\ f_1^i v_{1,2}^i + f_2^i v_{2,1}^i \end{bmatrix} \tag{8}$$

where the prime stands for the classical derivative ($f_i' = \frac{df_i}{dx}$), and $()_{,\alpha}$ for the partial derivative.

3.2. Formulation of the problem to be solved

The expression of the strain, Eq. (8), introduced in the problem in Eq. (4) yields a non-linear parametrized problem that is solved by an iterative process. In the present study, only one or two couples are built, i.e. $N = 1$ or 2. It is enough for the considered test cases.

The problem to be solved can be written as

$$a\left(\sum_{i=1}^{N} \mathbf{f^i} \circ \mathbf{v}^i, \delta \mathbf{u} \right) = 0, \quad \forall \, \delta \mathbf{u} \in \delta \mathcal{W} \tag{9}$$

The test function becomes

$$\delta\left(\sum_{i=1}^{N} \mathbf{f^i} \circ \mathbf{v}^i \right) = \sum_{i=1}^{N} \delta \mathbf{f^i} \circ \mathbf{v}^i + \sum_{i=1}^{N} \mathbf{f^i} \circ \delta \mathbf{v}^i \tag{10}$$

Introducing the test function defined by Eq. (10) into the weak form Eq. (9), the two following equations can be deduced:

- for the test function $\delta \mathbf{f}$

$$a\left(\sum_{i=1}^{N} \mathbf{v}^i \circ \mathbf{f^i}, \sum_{i=1}^{N} \mathbf{v}^i \circ \delta \mathbf{f^i} \right) = 0 \quad \forall \, \delta \mathbf{f} \tag{11}$$

- for the test function $\delta \mathbf{v}$

$$a\left(\sum_{i=1}^{N} \mathbf{f^i} \circ \mathbf{v}^i, \sum_{i=1}^{N} \mathbf{f^i} \circ \delta \mathbf{v}^i \right) = 0 \quad \forall \, \delta \mathbf{v} \tag{12}$$

From Eqs. (11) and (12), a coupled non-linear problem is derived. A

fixed point method is chosen to solve it. Starting from an initial function $(\widetilde{\mathbf{f}}^{(0)}, \widetilde{\mathbf{v}}^{(0)})$, we construct a sequence $(\widetilde{\mathbf{f}}^{(l)}, \widetilde{\mathbf{v}}^{(l)})$ which satisfy Eqs. (11) and (12) respectively. For each of them, an eigenfrequency/ eigenmode problem is solved. Only 1D or 2D functions have to be found, as the other one is assumed to be known (from the previous step of the fixed point strategy). So, the approach leads to the algorithm given in the Algorithm 1 where a iterative process is performed. The fixed point algorithm is stopped when the distance between two consecutive terms are sufficiently small.

Note that the initialization of the process is an important step of the algorithm. It will be discussed in the numerical examples. For $m_{mode} > 1$, the converged z-function $\mathbf{f}^1$ at the first stage is used for the next one. In the present approach, each eigensolution is obtained independently from the others to build the most accurate z-functions associated to the involved mode.

Algorithm 1 Algorithm

for $m_{mode} = 1$ to N_{mode} **do**
  Initialize $\widetilde{\mathbf{f}}^{(0)}$
  $l = 0$
  Compute m_{mode}^{th} eigenfrequency/eigenmode $\widetilde{\mathbf{v}}^{(l)}$ from Eq. (12), $\widetilde{\mathbf{f}}^{(0)}$ being known
  while $Err_{fixedPt} < \epsilon_{fp}$ **do**
    $l = l + 1$
    Compute p_{mode}^{th} eigenfrequency $\widetilde{\omega}_f^{(l)}$/eigenmode $\widetilde{\mathbf{f}}^{(l)}$ from Eq. (11), $\widetilde{\mathbf{v}}^{(l-1)}$ being known, p_{mode} such that $\widetilde{\omega}_f^{(l)}$ is the nearest eigenfrequency from $\widetilde{\omega}_v^{(l-1)}$.
    Compute p_{mode}^{th} eigenfrequency $\widetilde{\omega}_v^{(l)}$/eigenmode $\widetilde{\mathbf{v}}^{(l)}$ from Eq. (12), $\widetilde{\mathbf{f}}^{(l)}$ being known, p_{mode} such that $\widetilde{\omega}_v^{(l)}$ is the nearest eigenfrequency from $\widetilde{\omega}_f^{(l)}$.
  end while
  Set $\mathbf{f}^{m_{mode}} = \widetilde{\mathbf{f}}^{(l)}$
  Set $\mathbf{v}^{m_{mode}} = \widetilde{\mathbf{v}}^{(l)}$
  Set $\omega^{m_{mode}} = \widetilde{\omega}_v^{(l)}$
  Check for convergence
end for

3.3. Finite element discretization

In this section, the plate Finite Element approximation is presented for only one couple, i.e. $N = 1$, for convenience reasons. A classical finite element approximation in Ω and Ω_z for $(\mathbf{v}, \mathbf{f})$ is introduced. The elementary vector of degrees of freedom (dof) associated with one element Ω_e of the mesh in Ω is denoted $\mathbf{q}_e^v$. The elementary vector of dofs associated with one element Ω_{ze} of the mesh in Ω_z is denoted $\mathbf{q}_e^f$. The displacement fields and the strain field are determined from the values of $\mathbf{q}_e^v$ and $\mathbf{q}_e^f$ by

$$\mathbf{v}_e = \mathbf{N}_{xy} \mathbf{q}_e^v, \quad \mathscr{E}_v^e = \mathbf{B}_{xy} \mathbf{q}_e^v, \mathbf{f}_e = \mathbf{N}_z \mathbf{q}_e^f, \quad \mathscr{E}_f^e = \mathbf{B}_z \mathbf{q}_e^f \tag{13}$$

where

$$\mathscr{E}_v^{eT} = [v_1 \quad v_{1,1} \quad v_{1,2} \quad v_2 \quad v_{2,1} \quad v_{2,2} \quad v_3 \quad v_{3,1} \quad v_{3,2}]$$

$$\mathscr{E}_f^{eT} = [f_1 \quad f_1' \quad f_2 \quad f_2' \quad f_3 \quad f_3']$$

The matrices $\mathbf{N}_{xy}$, $\mathbf{B}_{xy}$, $\mathbf{N}_z$, $\mathbf{B}_z$ contain the interpolation functions, their derivatives and the jacobian components.

3.4. Finite element problem to be solved on Ω

For the sake of simplicity, the functions $\widetilde{\mathbf{f}}^{(l)}$ which are assumed to be known, will be denoted $\widetilde{\mathbf{f}}$. And the function $\widetilde{\mathbf{v}}^{(l)}$ to be computed will be denoted $\mathbf{v}$. The strains included in Eq. (12) are defined as

$$\varepsilon(\widetilde{f} \circ v) = \Sigma_{\mathbf{z}}(\widetilde{f}) \mathscr{E}_{\mathbf{v}} \tag{14}$$

with

$$\Sigma_z(\widetilde{f}) = \begin{bmatrix} 0 & \widetilde{f}_1 & 0 & 0 & 0 & 0 & 0 & 0 & 0 \\ 0 & 0 & 0 & 0 & 0 & \widetilde{f}_2 & 0 & 0 & 0 \\ 0 & 0 & 0 & 0 & 0 & 0 & \widetilde{f}_3' & 0 & 0 \\ 0 & 0 & 0 & 0 & \widetilde{f}_2' & 0 & 0 & 0 & \widetilde{f}_3 \\ \widetilde{f}_1' & 0 & 0 & 0 & 0 & 0 & 0 & \widetilde{f}_3 & 0 \\ 0 & 0 & \widetilde{f}_1 & 0 & \widetilde{f}_2 & 0 & 0 & 0 & 0 \end{bmatrix}$$

(15)

For convenience reasons, the displacement $\mathbf{u}$ is written under the form $\mathbf{u} = \mathbf{D_z}(\widetilde{f})\mathbf{v} = \begin{bmatrix} \widetilde{f}_1 & 0 & 0 \\ 0 & \widetilde{f}_2 & 0 \\ 0 & 0 & \widetilde{f}_3 \end{bmatrix}\mathbf{v}$

The variational problem defined on Ω from Eq. (12) is

$$\int_\Omega \delta\mathscr{E}_\mathbf{v}^T \mathbf{k}_z(\widetilde{f})\mathscr{E}_\mathbf{v} d\Omega - \omega^2 \int_\Omega \delta\mathbf{v}^T \mathbf{m}_z(\widetilde{f})\mathbf{v}d\Omega = 0$$

(16)

where

$$\mathbf{k}_z(\widetilde{f}) = \int_{\Omega_z} \Sigma_\mathbf{z}(\widetilde{f})^T \mathbf{C}\Sigma_\mathbf{z}(\widetilde{f})dz \quad \mathbf{m}_z(\widetilde{f}) = \int_{\Omega_z} \rho\mathbf{D_z}(\widetilde{f})^T\mathbf{D_z}(\widetilde{f})dz$$

(17)

The introduction of the finite element approximation Eq. (13) in the variational Eq. (16) leads to the eigenvalue/ eigenmode problem:

$$[\mathbf{K}_z(\widetilde{f}) - \omega^2 \mathbf{M}_z(\widetilde{f})]\mathbf{q}^v = 0$$

(18)

where

- $\mathbf{q}^v$ is the eigenvector of the nodal displacements, associated with the finite element mesh in Ω,
- $\mathbf{K}_z(\widetilde{f})$ is the mechanical stiffness matrix obtained by summing the elements' stiffness matrices $\mathbf{K}_z^e(\widetilde{f}) = \int_{\Omega_e} [\mathbf{B}_{xy}^T \mathbf{k}_z(\widetilde{f})\mathbf{B}_{xy}]d\Omega_e$
- $\mathbf{M}_z(\widetilde{f})$ is the mechanical mass matrix obtained by summing the elements' stiffness matrices $\mathbf{M}_z^e(\widetilde{f}) = \int_{\Omega_e} [\mathbf{N}_{xy}^T\mathbf{m}_z(\widetilde{f})\mathbf{N}_{xy}]d\Omega_e$

3.5. Finite element problem to be solved on Ω_z

As in the previous section, the known functions $\widetilde{\mathbf{v}}^{(l-1)}$ will be denoted $\widetilde{\mathbf{v}}$ and the functions $\widetilde{\mathbf{f}}^{(l)}$ to be computed will be denoted $\mathbf{f}$. The strain included in Eq. (11) is defined as

$$\varepsilon(\widetilde{v} \circ f) = \Sigma_{\mathbf{xy}}(\widetilde{v})\mathcal{E}_\mathbf{f}$$

(19)

where

$$\Sigma_{\mathbf{xy}}(\widetilde{v}) = \begin{bmatrix} \widetilde{v}_{1,1} & 0 & 0 & 0 & 0 & 0 \\ 0 & 0 & \widetilde{v}_{2,2} & 0 & 0 & 0 \\ 0 & 0 & 0 & 0 & 0 & \widetilde{v}_3 \\ 0 & 0 & 0 & \widetilde{v}_2 & \widetilde{v}_{3,2} & 0 \\ 0 & \widetilde{v}_1 & 0 & 0 & \widetilde{v}_{3,1} & 0 \\ \widetilde{v}_{1,2} & 0 & \widetilde{v}_{2,1} & 0 & 0 & 0 \end{bmatrix}$$

(20)

and the displacement is $\mathbf{u} = \mathbf{D_{xy}}(\widetilde{v})\mathbf{f} = \begin{bmatrix} \widetilde{v}_1 & 0 & 0 \\ 0 & \widetilde{v}_2 & 0 \\ 0 & 0 & \widetilde{v}_3 \end{bmatrix}\mathbf{f}$

The variational problem defined on Ω_z from Eq. (11) is

$$\int_{\Omega_z} \delta\mathscr{E}_\mathbf{f}^T \mathbf{k}_{xy}(\widetilde{v})\mathcal{E}_\mathbf{f}dz - \omega^2 \int_{\Omega_z} \delta\mathbf{f}^T\mathbf{m}_{xy}(\widetilde{v})\mathbf{f}d\Omega_z = 0$$

(21)

where $\mathbf{k}_{xy}(\widetilde{v})$ and $\mathbf{m}_{xy}(\widetilde{v})$ can be expressed under the following separated form:

$$\mathbf{k}_{xy}(\widetilde{v}) = \int_\Omega \Sigma_{\mathbf{xy}}(\widetilde{v})^T\mathbf{C}\Sigma_{\mathbf{xy}}(\widetilde{v})d\Omega \quad \mathbf{m}_{xy}(\widetilde{v}) = \int_\Omega \rho\mathbf{D_{xy}}(\widetilde{v})^T\mathbf{D_{xy}}(\widetilde{v})d\Omega$$

(22)

The introduction of the finite element discretization Eq. (13) in the variational Eq. (21) leads to the eigenvalue/eigenmode problem:

$$[\mathbf{K}_{xy}(\widetilde{v}) - \omega^2\mathbf{M}_{xy}(\widetilde{v})]\mathbf{q}^f = 0$$

(23)

where

- $\mathbf{q}^f$ is the vector of degree of freedom associated with the F.E. approximations in Ω_z.
- $\mathbf{K}_{xy}(\widetilde{v})$ is obtained by summing the elements' stiffness matrices:

$$\mathbf{K}_{xy}^e(\widetilde{v}) = \int_{\Omega_{ze}} [\mathbf{B}_z^T\mathbf{k}_{xy}(\widetilde{v})\mathbf{B}_z]dz_e$$

(24)

- $\mathbf{M}_{xy}(\widetilde{v})$ is obtained by summing the elements' mass matrices:

$$\mathbf{M}_{xy}^e(\widetilde{v}) = \int_{\Omega_{ze}} [\mathbf{N}_z^T\mathbf{m}_{xy}(\widetilde{v})\mathbf{N}_z]dz_e$$

(25)

4. Numerical results

In the numerical examples, an eight-node quadrilateral FE based on the classical Serendipity interpolation functions is used for the unknowns depending on the in-plane coordinates. For the unknowns depending on the z-coordinate, the displacement is described by a fourth-order interpolation as it is justified in [45]. A Gaussian numerical integration with 3×3 points is used to evaluate the elementary matrices. As far as the integration with respect to the transverse coordinate is concerned, an analytical integration is performed.

In this section, several numerical benchmark tests widely available in open literature [32] are presented in order to evaluate the accuracy of the present approach. Different cross-ply, angle-ply and sandwich plates, slenderness ratios and boundary conditions are considered to show the wide range of validity of the method.

The present approach, denoted VS-LD4, is compared with both reference solutions and other models available in open literature, see Table 1.

Note that only one couple is built for each test, unless otherwise mentioned.

4.1. Convergence study

The behavior of the present method is first illustrated on a cross-ply plate. The test case is described as follows:

Table 1
Models available in open literature and reference solutions.

LD4	It refers to the systematic work of Carrera and his "Carrera's Unified Formulation" (CUF), see [49,28,50]. A LayerWise model based on a displacement approach where each component is expanded until the fourth order is given; $12NC + 3$ unknown functions are used in this kinematic. It provides quasi-3D solution and could be considered as a reference solution.
3D FEM	3D FEM solution is also used as a reference solution. It is computed by the commercial code ANSYS using the quadratic 20-node brick element (SOLID146). 3D FEM Abaqus solutions are also provided in [51].
Exact solution	It can be found in [52,53].
Kant & Swaminathan 2001	It involves ESL model with a third-order expansion of each component of the displacements [54]. It is based on an analytical approach including 12 generalized unknowns.
Zhen et al. 2010	It is related to a global–local higher order shear deformation theory [55] involving 13 generalized unknowns. The continuity of the transverse shear stresses is fulfilled. It is based on an analytical approach. The stretching effect is not taken into account.
Kulkarni & Kapuria 2008	It refers to a third-order zigzag theory, denoted ZIGT [51], where the transverse shear stresses are continuous at the ply interfaces. 7 degrees of freedom per node are involved in this theory. The stretching effect is not taken into account.

Table 2

Fixed point convergence study – natural frequency $\bar{\omega}$ – square cross-ply plate – $a/h = 5 - NC = 1 - \alpha = 40 - N_x = N_y = 12$.

m_{mode}	Init. 1 – Bending modes					Init. 2 – in-plane modes			
	1,1	2,1	3,1	1,2	2,2	1 (AntiS[†])	1 (Sym[†])	2 (AntiS[†])	2 (Sym[†])
1	4.293	5.918	9.067	9.348	10.222	4.866	7.910	9.733	11.560
	4.075					4.866			
	4.075					4.866			
2		5.701					7.909		
		5.649					7.898		
		5.649					7.898		
3			8.864					9.733	
			8.659			.		9.733	
			8.659					9.733	
4				9.053					11.559
				8.916					11.549
				8.916					11.549
5					9.947				
		.			9.783				
					9.783				
LD4	4.075	5.649	8.659	8.916	9.783	4.867	7.898	9.733	11.549

[†] AntiS and Sym refer to Anti-symmetric and Symmetric modes, respectively.

Table 3

Convergence study – natural frequency $\bar{\omega}$ – square cross-ply plate – $a/h = 5 - NC = 6 - \alpha = 40$.

$N_x = N_y$	Modes			
	1,1	1,2/ 2,1	2,2	1,3
2	4.5399	8.7007	16.0726	16.3270
4	4.4798	8.2308	10.7975	12.5653
8	4.4769	8.1881	10.7034	12.3042
12	4.4767	8.1857	10.6996	12.2875
24	4.4767	8.1851	10.6987	12.2834
24 (LD4)	4.4767	8.1851	10.6987	12.2834

geometry: square cross-ply plate with length-to-thickness ratio $S = 5$, constituted of one or six layers, [0°], [0°/90°/0°/90°/0°/90°] respectively. All the layers have the same thickness.

boundary conditions: simply-supported plate

material properties: $E_1 = \alpha E_2$, $E_2 = E_3$, $\nu_{12} = \nu_{13} = \nu_{23} = 0.25$ $G_{12} = G_{13} = 0.6 E_2$, $G_{23} = 0.5 E_2$, $\rho^{(k)} = \rho_0 =$ constante

mesh: N_x, N_y are the number of elements along the x and y-axis, respectively.

results: the natural frequencies ω are normalized as $\bar{\omega} = 10 h \omega \sqrt{\rho_0 / E_2}$

reference values: LD4 model

In Table 2, two features of the method are shown: (i) the influence of the initialization, denoted Init. 1 and 2; (ii) the convergence of each fixed point associated to one vibration mode. For Init. 1, the initialization of the z-functions is such that in-plane displacements are linear and transverse one is constant through the thickness. This
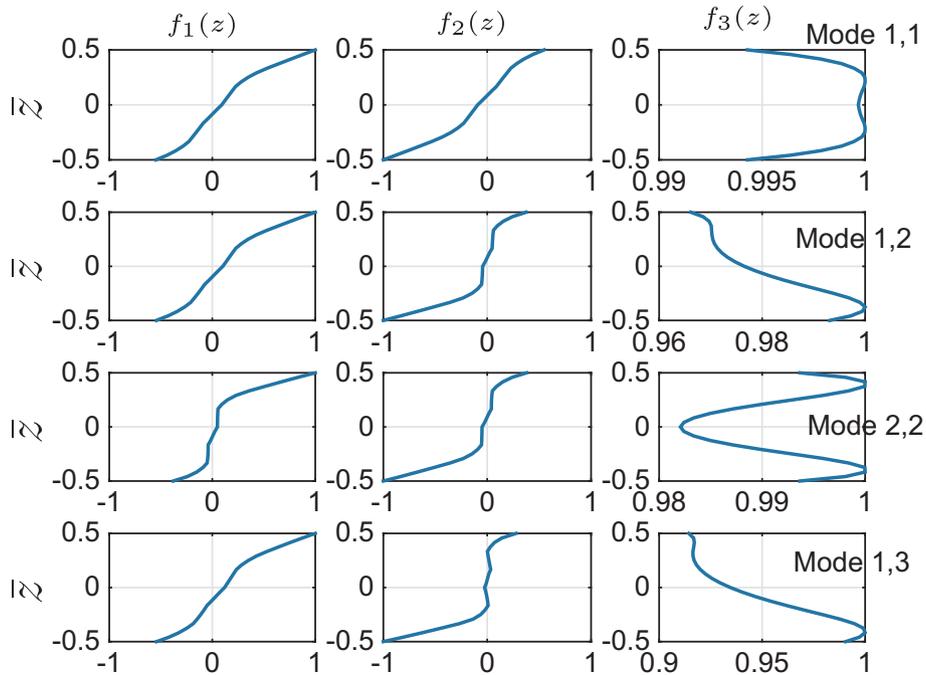

Fig. 2. $f_i(z)$ – square cross-ply plate – $a/h = 5 - NC = 6 - E_1/E_2 = 40$.

Table 4
Fundamental frequency $\bar{\omega}$ – square cross-ply plate – $a/h = 5$.

NC		E_1/E_2			
		10	20	40	100
2	VS-LD4	2.782	3.057	3.411	3.906
	LD4	2.782	3.057	3.411	3.906
	3D FEM	2.782	3.057	3.411	3.905
	exact	2.794	3.069	3.425	–
3	VS-LD4	3.265	3.695	4.092	4.530
	LD4	3.265	3.695	4.092	4.530
	3D FEM	3.265	3.695	4.092	4.530
	exact	3.284	3.824	4.300	–
4 (Sym)	VS-LD4	3.310	3.799	4.273	4.789
	LD4	3.310	3.799	4.273	4.789
	3D FEM	3.310	3.799	4.273	4.7897
	exact	3.258	3.762	4.272	–
6	VS-LD4	3.342	3.908	4.477	5.072
	LD4	3.342	3.908	4.477	5.072
	3D FEM	3.342	3.908	4.477	5.072
	exact	3.365	3.936	4.509	–
9	VS-LD4	3.408	4.005	4.603	5.234
	LD4	3.408	4.005	4.603	5.234
	3D FEM	3.408	4.005	4.603	5.233
	exact	3.443	4.055	4.668	–
10	VS-LD4	3.399	4.003	4.614	5.259
	LD4	3.399	4.003	4.614	5.259
	3D FEM	3.399	4.003	4.614	5.259
	exact	3.425	4.034	4.649	–

initialization corresponds to the CLT model with a 3D constitutive law. The five first bending modes are recovered and it must be denoted that the error between first and converged values are less than 5%. For Init. 2, a random initialization or a distribution such that the in-plane displacements are constant and the transverse one is linear through the thickness allow us to capture the in-plane modes. It should be noted that the convergence rate of each fixed point is high, as the correction of these functions is small. Only three or four iterations are sufficient to obtain a converged value of the eigenpulsations. Moreover, it can be concluded that the agreement with the LD4 model is very satisfactory.

A convergence study on the in-plane mesh is also carried out for the six layers configuration. From Table 3, it can be stated that the convergence rate is very good, a $N_x = N_y = 12$ mesh is sufficient to obtain the 5 first modes. The distribution of the z-functions f_i through the thickness is also given in Fig. 2 for 4 modes. We can notice that the f_3 functions associated to the modes 1,1 and 2,2 are nearly constant through the thickness, which is not the case for the modes 1,2 and 1,3. Thus, the correction of the z-functions is required to obtain accurate results. Indeed, using the f_3 function associated to the first mode for the three following ones leads to an error rate of 4.5, 5 and 8%, respectively ($\bar{\omega} = 8.5472$ (mode 1,2); $\bar{\omega} = 11.2488$ (mode 2,2); $\bar{\omega} = 13.2595$ (mode 1,3)).

4.2. Cross-ply multilayered composite plate

In this section, symmetric and anti-symmetric cross-ply laminated composite plates are considered with different number of layers and varying the E_1/E_2 ratio. The data is given as follows:

geometry: square cross-ply plate with length-to-thickness ratio $S = 5$, made of 2 to 10 layers (alternating orientation 0° and 90°, excepted for the four layers [0°/90°/90°/0°]). All the layers have the same thickness.
boundary conditions: simply-supported plate
material properties: same material as in Section 4.1
mesh: $N_x = N_y = 24$
results: the fundamental frequency ω is normalized as $\bar{\omega} = 10h\omega\sqrt{\rho_0/E_2}$
reference values: exact solution from [53] and 3D FEM solution computed by ANSYS with a refined converged mesh

The values of the fundamental frequency are summarized in Table 4 for each configuration. The present approach gives excellent results when compared to the LD4 and 3D FEM solutions, regardless of the degree of anisotropy and the number of layers. The separated representation does not affect the quality of the results.

Note that the exact solution can be different from the 3D FEM results with a maximum error rate of 4% ($NC = 3$, $E_1/E_2 = 40$). It seems that the results available in open literature are closed to the obtained 3D FEM results, see [55] for instance.

4.3. Sandwich plate [0°/90°/core/0°/90°]

In this section, the analysis of a non-symmetric sandwich plate is carried out. The ratio of anisotropy between the face and the core is high. The test is detailed below:

geometry: square sandwich plate with length-to-thickness ratios $S \in \{10, 100\}$. The thickness of each face sheet is $t_c = \frac{h}{10}$.
boundary conditions: simply-supported plate
material properties: Face sheets: $E_1 = 131$ GPa, $E_2 = E_3 = 10.34$ GPa, $\nu_{12} = \nu_{13} = 0.22$, $\nu_{23} = 0.49$,
$G_{12} = G_{23} = 6.895$ GPa, $G_{13} = 6.205$ GPa, $\rho_f = 1627$ kg/m³
Core (isotropic material): $E_1 = E_2 = E_3 = 6.89\ 10^{-3}$ GPa, $\nu_{12} = \nu_{13} = \nu_{23} = 0$,
$G_{12} = G_{23} = G_{13} = 3.45\ 10^{-3}$ GPa, $\rho_c = 97$ kg/m³
mesh: $N_x = N_y = 24$
results: the natural frequencies ω are normalized as $\bar{\omega} = \omega b^2/h\sqrt{\rho_f/E_{2f}}$
*reference values:* the exact solution is provided in [52].

The values of the six first natural frequencies are shown in Table 5

Table 5
Comparison of natural frequencies $\bar{\omega}$ – square sandwich plate [0°/90°/core/0°/90°].

S	Mode	VS-LD4	LD4	Kant & Swaminathan 2001	Zhen et al. 2010	Exact [52]
10	1,1	1.8492 (0.0)	1.8492 (0.0)	4.8594 (162)	1.9418 (5.1)	1.8480
	1,2	3.2227 (0.1)	3.2226 (0.1)	8.0187 (150)	3.3625 (4.4)	3.2196
	2,2	4.2941 (0.1)	4.2938 (0.1)	10.2966 (140)	4.4677 (4.1)	4.2894
	1,3	5.2341 (0.2)	5.2331 (0.2)	11.7381 (124)	5.4086 (3.5)	5.2236
	2,3	6.1056 (0.1)	6.1046 (0.1)	13.4706 (121)	6.3060 (3.5)	6.0942
	3,3	7.6933 (0.2)	7.6919 (0.2)	16.1320 (110)	7.9154 (3.1)	7.6762
100	1,1	11.9469 (0.0)	11.9457 (0.0)	15.5093 (30)	12.2374 (2.5)	11.9401
	1,2	23.4233 (0.1)	23.4144 (0.0)	39.0293 (67)	24.3213 (3.9)	23.4017
	2,2	30.9723 (0.1)	30.9608 (0.0)	54.7618 (77)	32.2539 (4.2)	30.9432
	1,3	36.1898 (0.1)	36.1664 (0.0)	72.7572 (101)	37.8300 (4.6)	36.1434
	2,3	41.4961 (0.1)	41.4744 (0.0)	83.4412 (101)	43.3893 (4.6)	41.4475
	3,3	49.0742 (1.4)	49.0363 (1.4)	105.3781 (111)	52.1795 (4.8)	49.7622

Table 6
Comparison of natural frequencies $\bar{\omega}$ for different t_c/t_f ratios – square sandwich plate [0°/90°/*core*/0°/90°] – $S = 10$.

t_c/t_f	VS-LD4	LD4	Kant & Swaminathan 2001	Zhen et al. 2010	Exact [52]
4	1.9092 (0.04)	1.9092 (0.04)	8.9948 (371)	1.9405 (1.7)	1.9084
10	1.8492 (0.06)	1.8492 (0.06)	4.8594 (162)	1.9418 (5)	1.8480
30	2.3341 (0.08)	2.3341 (0.08)	2.8481 (22)	2.5146 (7.8)	2.3321
50	2.5682 (0.09)	2.5682 (0.09)	2.8625 (11)	2.7777 (8.2)	2.5658

Table 7
Comparison of natural frequencies $\bar{\omega}$ for different boundary conditions – square sandwich plate [0°/90°/*core*/90°/0°] – $S = 5$.

	Mode	VS-LD4 (1 couple)	VS-LD4 (2 couples)	LD4	Abaqus 3D FEM [51]
CCCC	1,1	12.177 (1.0)	12.071 (0.2)	12.054 (0.1)	12.046
	1,2	18.462 (1.0)	18.324 (0.3)	18.285 (0.1)	18.270
	2,1	20.856 (1.3)	20.625 (0.2)	20.588 (0.1)	20.572
	2,2	25.174 (1.2)	24.943 (0.3)	24.895 (0.1)	24.873
	1,3	26.643 (0.9)	26.458 (0.2)	26.435 (0.1)	26.405
	3,1	30.962 (1.0)	30.722 (0.2)	30.673 (0.1)	30.644
	2,3	31.808	31.559	31.519	
	3,2	34.153	33.903	33.847	
CFCF		7.611 (0.9)	7.556 (0.1)	7.550 (0.1)	7.544
		9.450 (2.2)	9.261 (0.2)	9.246 (0.0)	9.241
		15.758 (1.0)	15.642 (0.2)	15.612 (0.1)	15.598
		17.655 (1.8)	17.383 (0.2)	17.353 (0.1)	17.340
		19.308 (1.9)	18.967 (0.1)	18.954 (0.0)	18.951
		23.920 (1.3)	23.637 (0.1)	23.609 (0.0)	23.598
CFFF		3.546 (3.9)	3.414 (0.1)	3.411 (0.0)	3.410
		4.785 (2.7)	4.663 (0.1)	4.660 (0.0)	4.658
		10.927 (3.5)	10.574 (0.2)	10.559 (0.0)	10.554
		13.030 (2.7)	12.696 (0.1)	12.682 (0.0)	12.677
		18.032 (2.2)	17.657 (0.0)	17.649 (0.0)	17.648
		18.986 (1.2)	18.796 (0.2)	18.754 (0.0)	18.743
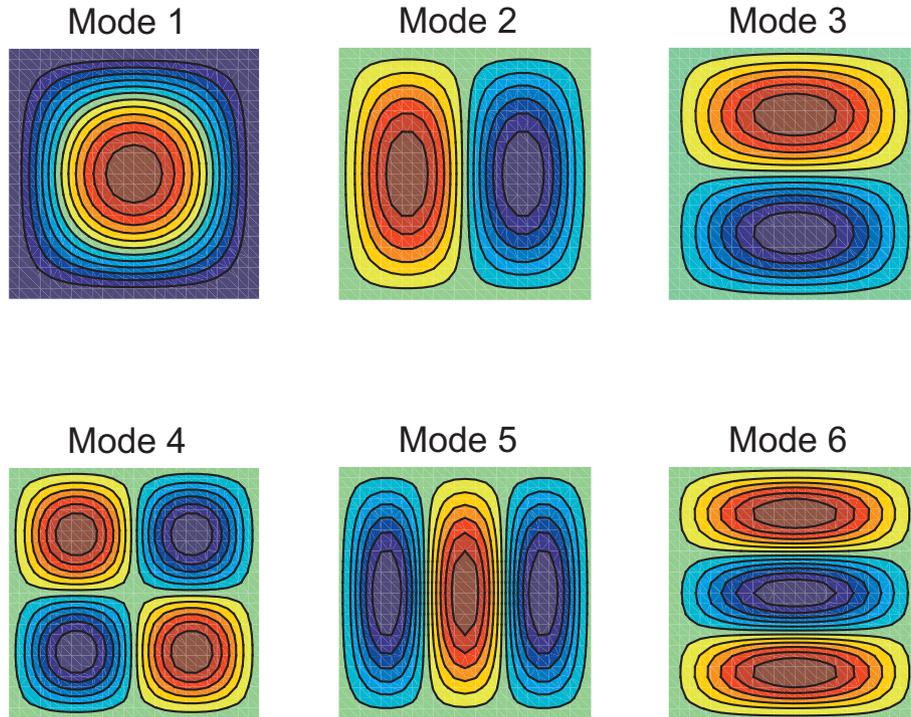
Fig. 3. 6 first modes – CCCC – square sandwich plate [0°/90°/*core*/90°/0°] – $S = 5$.

for both semi-thick and thin plates. Higher-order models fail to compute the eigenfrequencies, even for the thin case. The error rates vary from 3.1 to 162%. On the contrary, the LayerWise approaches, VS-LD4 and LD4, drives to results in excellent agreement with the exact solution.

The error rate is less than 1.4%. Once again, the results of these two models are very close.

Then, the influence of the core to face thickness ratio (t_c/t_f) is addressed in Table 6. The accuracy of the separated representation
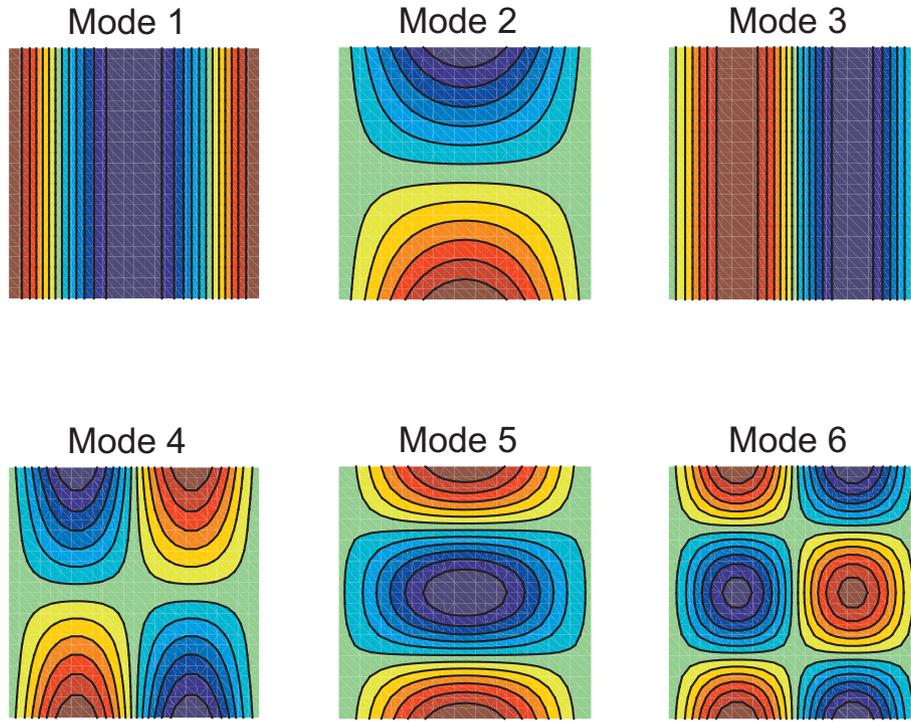
Fig. 4. 6 first modes – CFCF – square sandwich plate $[0°/90°/core/90°/0°]$ – $S = 5$.
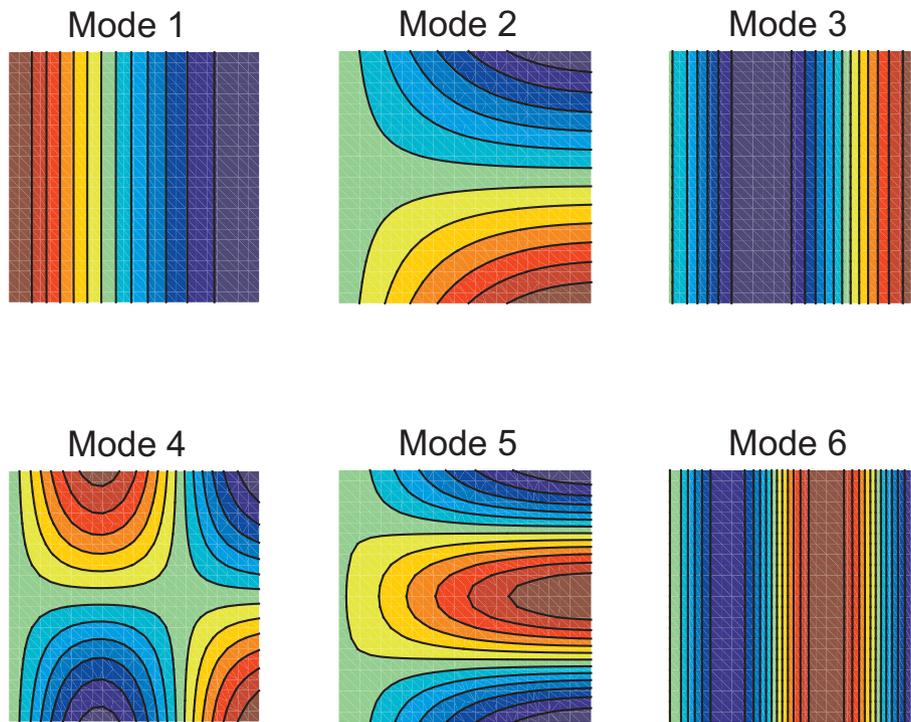
Fig. 5. 6 first modes – CFFF – square sandwich plate $[0°/90°/core/90°/0°]$ – $S = 5$.

Table 8
Comparison of natural frequencies $\bar{\omega}$ – square antisymmetric plate $[45°/-45°/45°/-45°]$ – $S = 5$ – simply-supported.

	Bending modes						In-plane modes	
VS-LD4 (1 couple)	13.09 (12.6)	21.18 (6.9)	29.70 (11)	32.57 (10)	32.57 (9)	36.81 (8)	17.20 (0.0)	34.41 (0.0)
VS-LD4 (2 couples)	11.84 (1.8)	20.29 (2.4)	27.03 (1.0)	29.99 (1.4)	30.87 (3.4)	35.16 (3.1)	17.20 (0.0)	34.41 (0.0)
LD4	11.64 (0.1)	19.82 (0.0)	26.75 (0.0)	29.58 (0.0)	29.86 (0.0)	34.22 (0.4)	17.20 (0.0)	34.41 (0.0)
ZIGT [51]	12.34 (6.1)	21.10 (6.5)	21.17 (21)	29.01 (1.9)	31.66 (6)	31.77 (6.8)	–	–
3D FEM	11.63	19.82	26.74	29.58	29.85	34.07	17.20	34.41

VS-LD4 (1 couple)	11.8749 (3.3)	19.3921 (2.3)	21.6647 (3.6)	26.3749 (1.8)	30.4527 (3.1)	31.4943 (3.0)	33.6048 (1.7)
VS-LD4 (2 couples)	11.6505 (1.3)	19.1149 (0.9)	21.0505 (0.6)	26.0109 (0.4)	29.6352 (0.3)	30.7069 (0.4)	33.1549 (0.3)
LD4	11.5114 (0.1)	18.9479 (0.0)	20.9186 (0.0)	25.9079 (0.0)	29.5423 (0.0)	30.5726 (0.0)	33.0976 (0.1)
3D FEM	11.4938	18.9435	20.9104	25.8993	29.5401	30.5642	33.0496

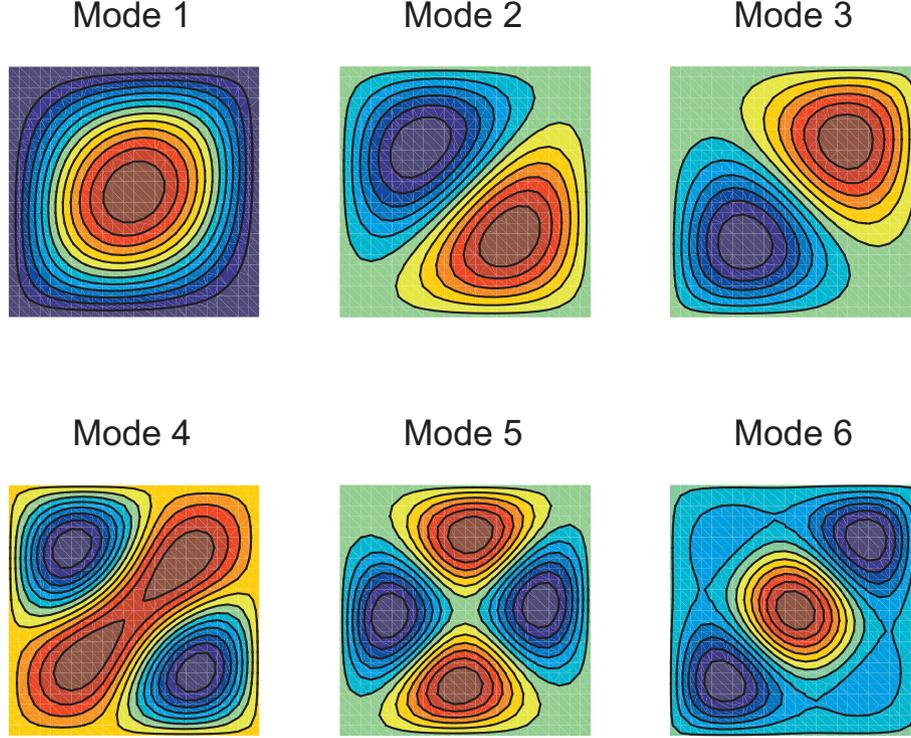## Mode 1

Mode 2

Mode 3

Mode 4

Mode 5

Mode 6

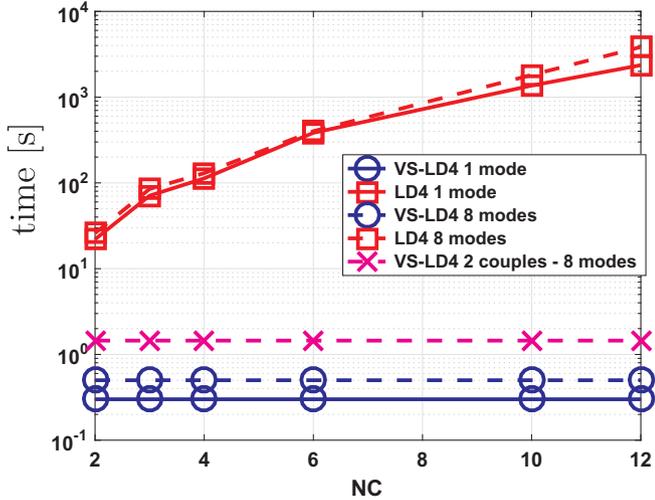**Fig. 6.** 6 first modes – $v_3^i(x, y)$ – square sandwich plate $[45°/-45°/-45°/45°]$ – $S = 5$.

Fig. 7. Computational cost with respect to the number of layers – $N_x = N_y = 24$.

approach is very satisfactory and does not depend on the geometry. The maximum error rate is 0.09%. The superiority of the LayerWise approach is also proved.

4.4. Different boundary conditions

In this section, different boundary conditions are considered for a symmetric sandwich plate. The configuration is summarized as:

geometry: square five-layer sandwich plate ($[0°/90°/core/90°/0°]$) with length-to-thickness ratios $S = 5$. The thickness of each face sheet is $\frac{h}{20}$.

boundary conditions: CCCC, CFCF, CFFF with C: Clamped, F: Free

material properties:

Face sheets: $E_1^f = 276$ GPa, $E_2^f = E_3^f = 6.9$ GPa, $\nu_{12}^f = \nu_{13}^f = 0.25$, $\nu_{23}^f = 0.3$,

$G_{12}^f = G_{23}^f = G_{13}^f = 6.9$ GPa, $\rho_f = 681.8$ kg/m^3

Core: $E_1^c = E_2^c = E_3^c = 5.776 \ 10^{-1}$ GPa, $\nu_{12}^c = \nu_{13}^c = \nu_{23}^c = 0.0025$,

$G_{12}^c = G_{13}^c = 1.079 \ 10^{-1}$ GPa, $G_{23}^c = 2.2215 \ 10^{-1}$ GPa, $\rho_c = 1000$ kg/m^3

mesh: $N_x = N_y = 24$

results: the natural frequency ω is normalized as $\bar{\omega} = 100\omega a \sqrt{\rho_f / E_2^f}$

reference values: 3D FEM Abaqus from [51]

The natural frequencies obtained with the VS-LD4, LD4 and 3D FEM models are given in Table 7 for the three types of boundary conditions. Using only one couple, the VS-LD4 approach drives to a maximum error rate of 3.9% (CFFF case). The CFFF test case seems to be the most difficult one. It is possible to reduce the error rate by building two simultaneous couples, the maximum error rate becomes only 0.3%.

For further illustration, the in-plane coordinates functions $v_3(x, y)$ corresponding to the 6 first eigenmodes are shown in Figs. 3–5 for the different boundary conditions. The modal analysis implies only bending modes.

4.5. Angle-ply multilayered composite plate

The method is assessed on other stacking sequences, namely

symmetric and anti-symmetric angle ply configurations. The test case comes from [51], it is described as follows:

geometry: square angle-ply plate with $S = 5$, $[45°/-45°/45°/-45°]$ and $[45°/-45°/-45°/45°]$ stacking sequences are involved. All the layers have the same thickness.
boundary conditions: simply-supported plate
material properties: same material as in Section 4.1
mesh: $N_x = N_y = 24$
results: the natural frequencies ω are normalized as $\bar{\omega} = S^2 h\omega\sqrt{\rho_0/E_2}$
reference values: 3D FEM solution computed by ANSYS

The six first bending modes and the two first in-planes ones of the anti-symmetric case are given in Table 8. The stacking sequence makes this example difficult for classical models. We can notice that even the refined model, ZIGT, fails to give accurate results (maximum error rate of 21%). On the contrary, a higher-order LayerWise model with a fourth-order expansion through the thickness is required. Concerning our approach, it should be noticed that only one couple is insufficient to have accurate results, excepted for the in-plane modes. For the bending modes, two couples allow us to obtain a good agreement with the reference solution. Note also that about 12 iterations of the fixed point algorithm are required to achieve the convergence. The results associated to the symmetric case is shown in Table 9. As expected, this case is simpler as the anti-symmetric one. One couple can be enough to have a satisfactory accuracy.

The in-plane functions $v_3^i(x, y)$ associated to the 6 first modes are presented in Fig. 6. The approach has the capability to capture all the bending modes oriented at 45°. Note that the modes 2 and 3 are not associated to the same natural frequency.

4.6. Computational costs

To further assess the present method, Fig. 7 gives the computational time to extract one or eight eigenfrequencies/eigenmodes with respect to the number of layers using Matlab software. Both the LD4 model and the method with the separated representation are compared. For this latter, all the resolutions due to the iterative process are included. The goal of this comparison is just to give an overall trend, but not an accurate cost, as the present method involves also the computation of some integrals over the domain Ω or Ω_z which do not exist for classical models (See Sections 3.4 and 3.5). It can be inferred from this figure that the cost of the VS-LD4 model does not depend on the number of layers. Thus, the gain will be high when *NC* increases. It should be also noticed that the computation of 2 simultaneous couples does not affect the efficiency of this process.

5. Conclusion

In this article, the modeling of composite plates is carried out for the free vibration analysis through a variable separation method. The results are assessed with various representative benchmarks by comparing with reference solutions. It is shown that the initialization of the iterative process has an important influence to capture the different modes. Accurate results are obtained for cross-ply, angle-ply and sandwich configurations involving different slenderness ratios, degree of anisotropy and boundary conditions. Layerwise approach is needed for some of them to achieve a good level of accuracy. It is also shown that few couples are sufficient. Finally, the computational cost of the present approach is lower than the classical Layerwise model.

Declaration of Competing Interest

The authors declare that they have no known competing financial interests or personal relationships that could have appeared to influence the work reported in this paper.

References

[1] Mindlin R. Influence of rotatory inertia and shear on flexural motions of isotropic, elastic plates. J Appl Mech ASME 1951;18:31–8.

[2] Ferreira A, Roque C, Jorge R. Free vibration analysis of symmetric laminated composite plates by FSDT and radial basis functions. Comput Methods Appl Mech Eng 2005;194:4265–78.

[3] Reddy J, Phan N. Stability and vibration of isotropic, orthotropic and laminated plates according to a higher order shear deformation theory. J Sound Vib 1985;98:157–70.

[4] Reddy J. A simple higher-order theory for laminated composite plates. J Appl Mech ASME 1984;51(4):745–52.

[5] Bhimaraddi A, Stevens L. A higher order theory for free vibration of orthotropic, homogeneous, and laminated rectangular plates. J Appl Mech ASME 1984;51:195–8.

[6] Soldatos K, Timarci T. A unified formulation of laminated composite, shear deformable, five-degrees-of-freedom cylindrical shell theories. Compos Struct 1993;25(1–4):165–71.

[7] Polit O, Touratier M. High order triangular sandwich plate finite element for linear and nonlinear analyses. Comput Methods Appl Mech Eng 2000;185:305–24.

[8] Reddy J. Mechanics of laminated composite plates and shells – theory and analysis. CRC Press Inc.; 2004.

[9] Vidal P, Polit O. A family of sinus finite elements for the analysis of rectangular laminated beams. Compos Struct 2008;84:56–72. https://doi.org/10.1016/j.compstruct.2007.06.009.

[10] Carrera E. On the use of the murakami's zig-zag function in the modeling of layered plates and shells. Comput Struct 2004;82:541–54.

[11] Lo K, Christensen R, Wu F. A higher-order theory of plate deformation. Part ii: Laminated plates. J Appl Mech ASME 1977;44:669–76.

[12] Tessler A, Saether E, Tsui T. Vibration of thick laminated composite plates. J Sound Vib 1995;179:475–98.

[13] Kapuria S, Nath J. On the accuracy of recent global-local theories for bending and vibration of laminated plates. Compos Struct 2013;95:163–72.

[14] Reddy J. A generalisation of two-dimensional theories of laminated composite plates. Commun Appl Numer Methods 1987;3:173–80.

[15] Robbins D, Reddy J. Modeling of thick composites using a layerwise laminate theory. Int J Numer Meth Eng 1993;36:655–77.

[16] Ferreira A, Roque C, Jorge R, Kansa E. Static deformations and vibration analysis of composite and sandwich plates using a layerwise theory and multiquadrics discretizations. Eng Anal Bound Elem 2005;29:1104–14.

[17] Kulikov G, Plotnikova S. Exact 3d stress analysis of laminated composite plates by sampling surfaces method. Compos Struct 2012;94:3654–63.

[18] Desai Y, Ramtekkar G, Shah A. Dynamic analysis of laminated composite plates using a layer-wise mixed finite element model. Compos Struct 2003;59:237–49.

[19] Carrera E. Theories and finite elements for multilayered plates and shells: a unified compact formulation with numerical assessment and benchmarking. Appl Mech Rev 2003;10(3):215–96.

[20] Demasi L. ∞^3 plate theories for thick and thin plates: the generalized unified formulation. Compos Struct 2008;84:256–70.

[21] Demasi L. $infty^6$ mixed plate theories based on the generalized unified formulation. Part i: governing equations. Compos Struct 2009;87(3):1–11.

[22] D'Ottavio M. A sublaminate generalized unified formulation for the analysis of composite structures. Comput Struct 2016;142:187–99.

[23] Murakami H. Laminated composite plate theory with improved in-plane responses. J Appl Mech ASME 1986;53:661–6.

[24] Vidal P, Polit O. Vibration of multilayered beams using sinus finite elements with transverse normal stress. Compos Struct 2010;92:1524–34. https://doi.org/10.1016/j.compstruct.2009.10.009.

[25] Tessler A, Sciuva MD, Gherlone M. A consistent refinement of first-order shear deformation theory for laminated composite and sandwich plates using improved zigzag kinematics. J Mech Mater Struct 2010;5:341–67.

[26] Cosentino PWE. An enhanced single-layer variational formulation for the effect of transverse shear on laminated orthotropic plates. Eur J Mech A Solids 2010;29(4):567–90.

[27] Vidal P, Polit O. A refined sinus plate finite element for laminated and sandwich structures under mechanical and thermomechanical loads. Comput Methods Appl Mech Eng 2013;253:396–412.

[28] Carrera E. Historical review of zig-zag theories for multilayered plates and shells. Appl Mech Rev 2003;56(3):287–308.

[29] Noor A, Burton W. Assessment of computational models for multilayered composite shells. Appl Mech Rev 1990;43(4):67–97.

[30] Zhang Y, Yang C. Recent developments in finite elements analysis for laminated composite plates. Compos Struct 2009;88:147–57.

[31] Carrera E, Brischetto S. A survey with numerical assessment of classical and refined theories for the analysis of sandwich plates. Appl Mech Rev 2009;62.

[32] Sayyad A, Ghugal Y. On the free vibration analysis of laminated composite and sandwich plates: a review of recent literature with some numerical results. Compos Struct 2015;129:177–201.

[33] Kerr A. An extension of the kantorovich method. Quart Appl Math 1968;26:219–29.

[34] Kerr A. An extended kantorovich method for the solution of eigenvalue problems. Int J Solids Struct 1969;5:559–72.

[35] Shufrin I, Eisenberger M. Stability and vibration of shear deformable plates first order and higher order analyses. Int J Solids Struct 2005;42:1225–51.

[36] Shufrin I, Eisenberger M. Semi-analytical modeling of cutouts in rectangular plates with variable thickness – free vibration analysis. Appl Math Modell

2016;40(15):6983–7000. https://doi.org/10.1016/j.apm.2016.02.020.

[37] Singhatanadgid P, Singhanart T. The kantorovich method applied to bending, buckling, vibration, and 3d stress analyses of plates: a literature review. Mech Adv Mater Struct 2005. https://doi.org/10.1080/15376494.2017.1365984.

[38] Ladevèze P. Nonlinear computational structural mechanics – new approaches and non-incremental methods of calculation. Springer-Verlag; 1999.

[39] Chinesta F, Ammar A, Leygue A, Keunings R. An overview of the proper generalized decomposition with applications in computational rheology. J Non-Newton Fluid Mech 2011;166(11):578–92.

[40] Chinesta F, Ammar A, Cueto E. Recent advances and new challenges in the use of the proper generalized decomposition for solving multidimensional models. Arch Comput Methods Eng 2010;17(4):327–50.

[41] Ammar A, Mokdada B, Chinesta F, Keunings R. A new family of solvers for some classes of multidimensional partial differential equations encountered in kinetic theory modeling of complex fluids. J Non-Newton Fluid Mech 2006;139:153–76.

[42] Savoia M, Reddy J. A variational approach to three-dimensional elasticity solutions of laminated composite plates. J Appl Mech ASME 1992;59:166–75.

[43] Bognet B, Bordeu F, Chinesta F, Leygue A, Poitou A. Advanced simulation of models defined in plate geometries: 3D solutions with 2D computational complexity. Comput Methods Appl Mech Eng 2012;201–204:1–12. https://doi.org/10.1016/j.cma.2011.08.025.

[44] Vidal P, Gallimard L, Polit O. Assessment of a composite beam finite element based on the proper generalized decomposition. Compos Struct 2012;94(5):1900–10. https://doi.org/10.1016/j.compstruct.2011.12.016.

[45] Vidal P, Gallimard L, Polit O. Proper generalized decomposition and layer-wise approach for the modeling of composite plate structures. Int J Solids Struct 2013;50(14–15):2239–50. https://doi.org/10.1016/j.ijsolstr.2013.03.034.

[46] Vidal P, Gallimard L, Polit O. Shell finite element based on the proper generalized decomposition for the modeling of cylindrical composite structures. Comput. Struct. 2014;132:1–11. https://doi.org/10.1016/j.compstruc.2013.10.015.

[47] Ammar A, Chinesta F. Circumventing the curse of dimensionality in the solution of highly multidimensional models encountered in quantum mechanics using mesh-free finite sums decompositions. Lecture Notes Comput Sci Eng 2006;65:1–17.

[48] Cances E, Ehrlacher V, Lelièvre T. Greedy algorithms for high-dimensional eigen-value problems. Constr Approx 2014;40(3):387–423.

[49] Carrera E. Developments, ideas and evaluations based upon the reissner's mixed theorem in the modeling of multilayered plates and shells. Appl Mech Rev 2001;54:301–29.

[50] D'Ottavio M, Ballhause D, Wallmersperger T, Kröplin B. Considerations on higher-order finite elements for multilayered plates based on a unified formulation. Comput Struct 2006;84:1222–35.

[51] Kulkarni S, Kapuria S. Free vibration analysis of composite and sandwich plates using an improved discrete kirchhoff quadrilateral element based on third-order zigzag theory. Comput Mech 2008;42(6):803–24.

[52] Rao M, Scherbatiuk K, Desai Y, Shah A. Natural vibrations of laminated and sandwich plates. J Eng Mech ASCE 2004;130:1268–78.

[53] Noor A. Free vibrations of multilayered composite plates. AIAA J 1973;11:1038–9.

[54] Kant T, Swaminathan K. Analytical solutions for free vibration of laminated composite and sandwich plates based on a higher-order refined theory. Compos Struct 2001;53:73–85.

[55] Zhen W, Wanji C, Xiaohui R. An accurate higher-order theory and c0 finite element for free vibration analysis of laminated composite and sadwich plates. Compos Struct 2010;92:1299–307.